
Article:
Eachus, H., Zaucker, A., Oakes, J.A. et al. (11 more authors) (2017) Genetic disruption of 21-hydroxylase in zebrafish causes interrenal hyperplasia. Endocrinology, 158 (12). pp. 4165-4173. ISSN 0013-7227

https://doi.org/10.1210/en.2017-00549

Genetic disruption of 21-hydroxylase in zebrafish causes interrenal hyperplasia

Helen Eachus, Andreas Zaucker, James A Oakes, Aliesha Griffin, Meltem Weger, Tülay Güran, Angela Taylor, Abigail Harris, Andy Greenfield, Jonathan L Quanson, Karl-Heinz Storbeck, Vincent T Cunliffe, Ferenc Müller, Nils Krone

Endocrinology
Endocrine Society

Submitted: June 13, 2017
Accepted: September 07, 2017
First Online: September 13, 2017

An *in vivo* model of 21-hydroxylase deficiency

Genetic disruption of 21-hydroxylase in zebrafish causes interrenal hyperplasia

Helen Eachus[1], Andreas Zaucker[2], James A Oakes[1,6], Aliesha Griffin[2], Meltem Weger[2], Tülay Güran[2], Angela Taylor[2], Abigail Harris[3], Andy Greenfield[3], Jonathan L Quanson[4], Karl-Heinz Storbeck[4], Vincent T Cunliffe[1], Ferenc Müller[5], Nils Krone[1, 6]

[1] *The Bateson Centre, Department of Biomedical Science, Firth Court, Western Bank, Sheffield S10 2TN, United Kingdom*

[2] *Centre for Endocrinology, Diabetes, and Metabolism, College of Medical and Dental Sciences, University of Birmingham, Birmingham, B15 2TT, United Kingdom*

[3] *Mammalian Genetics Unit, Medical Research Council, Harwell Institute, Oxfordshire, OX11 0RD, United Kingdom*

[4] *Department of Biochemistry, Stellenbosch University, Stellenbosch, 7602, Matieland, South Africa*

[5] *Institute of Cancer and Genomic Sciences, University of Birmingham, College of Medical and Dental Sciences, Birmingham, United Kingdom, Birmingham, B15 2TT, United Kingdom*

[6] *Academic Unit of Child Health, Department of Oncology and Metabolism, University of Sheffield, Sheffield S10 2TG, United Kingdom*

Received 13 June 2017. Accepted 07 September 2017.

Congenital adrenal hyperplasia is a group of common inherited disorders leading to glucocorticoid deficiency. Most cases are caused by 21-hydroxylase deficiency (21OHD). The systemic consequences of imbalanced steroid hormone biosynthesis due to severe 21OHD remains poorly understood. Therefore, we have developed a zebrafish model for 21OHD, which focuses on the impairment of glucocorticoid biosynthesis. A single 21-hydroxylase gene (*cyp21a2*) is annotated in the zebrafish genome based on sequence homology. Our *in silico* analysis of the Cyp21a2 protein sequence suggests a sufficient degree of similarity for the usage of zebrafish *cyp21a2* to model aspects of human 21OHD *in vivo*. We determined the spatio-temporal expression patterns of *cyp21a2* by whole mount *in situ* hybridisation and RT-PCR throughout early development. Early c*yp21a2* expression is restricted to the interrenal gland (zebrafish adrenal counterpart) and the brain. To further explore the *in vivo* consequences of 21-hydroxylase deficiency we created several *cyp21a2* null-allele zebrafish lines employing a transcription activator-like effector nuclease genomic engineering strategy. Homozygous mutant zebrafish larvae showed an upregulation of the hypothalamic-pituitary-interrrenal axis and interrenal hyperplasia. Furthermore, Cyp21A2-deficient larvae had a typical steroid profile with reduced concentrations of cortisol and increased concentrations of 17-hydroxyprogesterone and 21-deoxycortisol. Affected larvae showed an upregulation of the hypothalamic-pituitary-interrrenal axis and interrenal hyperplasia. Downregulation of the glucocorticoid-responsive genes *pck1* and *fkbp5* indicated systemic glucocorticoid deficiency. Our work demonstrates the crucial role of Cyp21a2 in glucocorticoid biosynthesis in zebrafish larvae and establishes a novel *in vivo* model allowing for studies of systemic consequences of altered steroid hormone synthesis.

Zebrafish larvae with disrupted 21-hydroxylase have interrenal hyperplasia and systemic glucocorticoid deficiency.

Introduction

Steroid hormones are key regulators of sex development, behavior, body homeostasis and metabolism. Deficiencies of steroid hormone synthesis and action are common causes of

disorders of sex development (DSD) including congenital adrenal hyperplasia (CAH). CAH ranks amongst the most common inherited metabolic endocrine disorders occurring in about 1 in 10,000 to 1 in 15,000 affected individuals (1,2). It is associated with significant morbidity and mortality (3,4) and represents a classic example of conditions with severe systemic consequences due to altered steroid hormone synthesis. The majority of CAH cases are caused by 21-hydroxylase (CYP21A2) deficiency resulting from inactivating mutations in the *CYP21A2* gene. CYP21A2 is a cytochrome P450 enzyme located in the endoplasmic reticulum, which in humans catalyzes the conversion of 17-hydroxyprogesterone to 11-deoxycortisol, a cortisol precursor, and the conversion of progesterone to 11-deoxycorticosterone, a precursor of aldosterone in humans (2). Disruption of this pathway renders patients unable to synthesize cortisol efficiently and results in the overproduction of ACTH by the pituitary due to diminished negative feedback. The stimulation of the adrenal cortex by ACTH in turn leads to the overproduction of cortisol precursors, which are diverted to the biosynthesis of sex hormones leading to sex hormone excess.

The major challenge in the field of steroid endocrinology is a substantial lack of understanding of systemic consequences of genetically disrupted steroid hormone synthesis causing CAH. Increasing evidence suggested that steroid hormone precursors altered in inborn errors of steroidogenesis such as 21-hydroxylase deficiency can alter glucocorticoid action (5). However, the homeostatic consequences on the whole organism remain elusive. While, a murine model of 21-hydroxylase deficiency due to naturally occurring mutations (6) has led to novel insights of adrenal development (7,8), only limited insights regarding systemic effects of altered steroid synthesis on the whole organism have been gained due to difficulties maintaining these mice.

Zebrafish are a comprehensive *in vivo* model organism for studying adrenal steroid hormone biosynthesis (9-11). Importantly, zebrafish share extensive homologies with humans in terms of their genome, the structure and function of several neural and physiological systems, including the neuroendocrine axis (12). In contrast to mice, zebrafish generate cortisol as the main glucocorticoid, with the same intermediates as humans and, as day active animals, follow a similar circadian rhythm (13). Thus, we anticipate zebrafish to represent a highly suitable model organism to explore systemic consequences of genetically altered steroid hormone biosynthesis.

Only very limited information is available on zebrafish 21-hydroxylase (cyp21a2) despite the well-recognised biosynthesis of cortisol in zebrafish (14) for which a 21-hydroxylation step is crucially required. Therefore, we have developed a novel cyp21a2-deficient zebrafish model employing a transcription activator-like effector nucleases (TALENs) strategy to define the role of zebrafish 21-hydroxylase. Cyp21a2-deficient zebrafish have a significant number of systemic hallmark features of human 21-hydroxylase deficiency including upregulation of the hypothalamic-pituitary-interrenal axis, interrenal hyperplasia, pathognomonic steroid hormone profiles and reduced systemic glucocorticoid medicated expression of target genes. Thus, we believe that this model will not only define crucial steps of the steroidogenic pathway in zebrafish, but also serve as a model to delineate systemic effects of glucocorticoid deficiency specific to 21-hydroxylase deficiency.

Materials and methods

Zebrafish husbandry

Zebrafish were maintained in a recirculating system (ZebTECTM, Tecniplast®, Kettering, UK, and Sheffield, UK) at 28.5 °C in a 10:14 dark: light photoperiod. Embryos were obtained by natural spawning and incubated at 28.5 °C in E3 medium (5 mmol/L NaCl, 0.17 mmol/L KCl, 0.33 mmol/L CaCl2, 0.33 mmol/L $MgSO_4$) containing 2 µg/mL gentamycin. The developmental stages were determined according to hours post-fertilisation (hpf) and

morphological features as previously described (15). All procedures were approved by the Home Office, United Kingdom and carried out line with the Animals (Scientific Procedures) Act 1986.

Comparison of vertebrate 21-hydroxylase protein sequences

CYP21A2 protein sequences were retrieved from the National Center for Biotechnology Information (NCBI): NP_000491.4 [*Homo sapiens*, Human], XP_003311237.1 [*Pan troglodytes*, Chimpanzee], NP_001181556.1 [*Macaca mulatta*, Macaque], NP_001003335.1 [*Canis lupus familiaris*, Dog], NP_001013614.1 [*Bos Taurus*, Cattle], NP_034125.2 [*Mus musculus*, Mouse], NP_476442.2 [*Rattus norvegicus*, Rat], NP_001092828.1 [*Gallus gallus*, Chicken], XP_002941314.2 [*Xenopus (Silurana) tropicalis*, Frog], XP_009290467.1 [*Danio rerio*, Zebrafish]. Multiple sequence alignments were carried out using the online tool Clustal Omega (*www.ebi.ac.uk/Tools/msa/clustalo)*(16,17) with the default settings.

Gene expression analysis by RT-PCR

Total RNA was extracted and cDNA synthesised as previously described (18). 100 ng of cDNA was used as template in 20 µl PCR reactions set up in MegaBlue Mastermix (Microzone), including 300 nM for each *cyp21a2* primer. The cycler programme consisted of an initial activation at 94 °C for 2 min followed by 36 cycles of 94 °C for 30 s, 60 °C for 30 s and 72 °C for 30 s, before a final elongation for 10 min at 72 °C. The whole PCR reaction was loaded for analysis on a 2% agarose gel. No template controls (NTCs) and a PCR reaction with a *cyp21a2* CDS containing pGEMT-easy vector (Promega) served as negative and positive controls, respectively.

Whole-mount RNA-in situ hybridization (WISH)

WISH was carried out following a standard protocol as previously described (19). For the generation of *cyp21a2* probes, a pGEMT-easy vector (Promega) containing the *cyp21a2* cDNA (ENSDART00000150512) was cut with NdeI and SacII restriction enzymes to generate templates for *in vitro* transcription. Digoxigenin labelled *cyp21a2* sense and antisense probes were then synthesized by *in vitro* transcription of 1 µg template with T7 (NdeI, sense) and SP6 (SacII, anti-sense) polymerases using the reagents of the *DIG RNA Labeling Kit* (11175025910, Roche).

For the generation of the *cyp17a2* probe, a 996 bp fragment of the *cyp17a2* transcript (NM_001105670.1) was amplified from 3 dpf AB wild type cDNA using the primer pair: Forward: GGCTGACAGTCTGTGTGAGG and Reverse: GTGTAGCGCTCAGGCTGTAA. The PCR product was cloned into pGEMT-easy vector and the insert was sequenced. The *cyp17a2* probe was generated using T7/NdeI for sense and SP6/NcoI for the anti-sense probe. The *pomca* probe was generated as previously described (20).

Generation of cyp21a2 mutants by Transcription activator-like effector nucleases (TALEN)

The pair of TALENs targeting exon2 of the *cyp21a2 gene* was generated using the Golden Gate TALEN kit (Addgene, Cambridge, MA). TALEN target sites were determined by TAL effector Nucleotide Targeter Version. 2.0 (21). The sequences of the repeat-variable di-residues (RVD) in the TAL Effector DNA-binding domains were: RVD TALE1 (left):NG-HD-NG-NH-NH-NG-HD-HD-NG-HD-NH-HD-NG-HD-NG-HD and RVD TALE2 (right): NG-NH-NH-NH-HD-NH-NI-NH-NI-NG-HD-HD-NI-NH-HD-NI-NG-NH-NG. TALEN mRNA was synthesized using SP6 polymerase mMessage machine kit (Life Technologies) after digesting 1 µg of plasmid DNA with NotI.

TALENs were injected into one cell stage embryos, using 1 nl of injection solution, containing 50 or 150 ng/µl of each TALEN diluted in Nuclease free water (Promega) plus 0.1% Phenol Red. F0 generations were grown to adulthood from the injected embryos and screened for transmission of *cyp21a2* mutations. Identified founders were outcrossed to fish to generate F1 generations. The F1 generation fish were screened for heterozygous *cyp21a2*

mutations. F1 fish with defined *cyp21a2* mutant alleles were outcrossed to their respective genetic backgrounds to generate the F2 generation. The heterozygous mutant fish of the F2 generation were in-crossed to study *cyp21a2* mutant phenotypes in embryos and larvae.

Genotyping cyp21a2 mutants

Genomic DNA was extracted either from fin clips or whole larvae. For the extraction of genomic DNA, samples were lysed in 20 µl (embryos) to 40 µl (fin clips) of RAPID-PCR buffer. PCR amplification of *cyp21a2* exon2 was carried out in 20 µl PCR-reactions using 300 nM of each primer (Forward: CTCTCGTGGGCTAAACAAGC and Reverse: ACATGTATCCACCATTTGCG) and 1 µl genomic DNA template in MegaBlue mix (Microzone). The PCR programme consisted of an initial activation at 94 °C for 2 min followed by 36 cycles of 94 °C for 30 s, 58 °C for 30 s and 72 °C for 30 s, before a final elongation for 10 min at 72 °C. Ten µl PCR product was then digested with BseYI in a 30 µl reaction. The digests were analysed on a 1% agarose gel. The 179 bp product is cleaved in wild type samples only, giving 103 bp and 76bp products (**Supplementary Figure 1**).

Analysis of visual background adaptation (VBA)

Zebrafish larvae can adjust their pigmentation to match their surrounding environments: a form of crypsis. To identify *cyp21a2* mutants, larvae were sorted according to VBA response at 96 hpf. The assay was carried out as previously described (18).

Area measurements on images from WISH

Larvae derived from in-crosses of adult *cyp21a2*$^{UOB2122/+}$ and *cyp21a2*$^{UOB2123/+}$ fish were raised to 120 hpf, at a density of around 100 larvae per petri dish (20 ml). Ten VBA+ larvae and ten VBA- siblings were fixed and processed through *cyp17a2* WISH together in one 1.5 ml tube. Images depicting a dorsal view of the interrenal gland for individual larvae after WISH were cropped and arranged using Adobe Photoshop. ImageJ software was used to set a colour threshold in order to distinguish background from the dark purple WISH staining. The number of stained pixels were then quantified using ImageJ.

Induction of osmotic stress

Sodium chloride treatments of 250 mM (in E3) were given at 120 hpf for 20 minutes.

Steroid hormone measurements

After the washing of chemical treatments, each clutch of 150 larvae was then transferred into a silanised test tube and snap frozen on dry ice. One ml of PBS was added to the sample and the cells were lysed via four rounds of freeze thawing. After the lysis the samples were homogenised with a pestle homogeniser. Twenty µl of a solution containing a mix of deuterated steroids in MeOH were added to the samples to provide an internal reference for normalisation. A calibration series of a mix of steroids was generated in 50% MeOH. Steroids were extracted from the samples with 3 ml Methyl tert-butyl ether (MTBE). The upper MTBE phase with the extracted steroids was transferred into clean glass test. The extraction step was repeated using an additional 3 ml MTBE. The upper MTBE phase was added to the extract from first round of extraction and the pooled solvent evaporated under a stream of nitrogen. The dried steroids were subsequently resuspended in 150 µl 50% Methanol and were separated and quantified using an ACQUITY UPLC system (Waters, Milford, USA) coupled to Xevo TQ-S tandem mass spectrometer (Waters, Milford, USA). Chromatographic separation was achieved using a UPLC high strength silica (HSS) T3 column (2.1 mm x 50 mm, 1.8 µm) (Waters, Milford, USA) as previously described (22).

Comparative gene expression analysis by qPCR

At 120 hpf, clutches of 30 VBA+ and 30 VBA- larvae were snap frozen in liquid nitrogen. Total RNA was extracted and reverse transcribed as described above. Quantitative PCR methods and primers sequences for *pomca*, *fkbp5* and *pck1* have been previously described

(18). Expression levels for each gene were normalised to *gapdh* and fold change values were generated relative to wild type control levels. Biological replicates were standardised as previously described (23).

Optical Projection Tomography

Samples were embedded in 1% agarose in water, dehydrated for 24 hours in 100% MeOH and then cleared with BABB (1:2, benzyl alcohol:benzyl benzoate) for 48 hours. Samples were imaged with a bespoke Optical Projection Tomography (OPT) scanner (24) with white light, followed by UV light. Scans were reconstructed with NRecon (Bruker microCT), and further processed in Fiji to generate 3D images.

Statistical analysis

Statistical analyses and graphics were prepared using 'R' version 3.3.0. For the comparison of means between two samples, unpaired t-tests were used to test for significant differences. For the comparison of means of more than two samples, one- or two-way Analysis Of Variance (ANOVA) was used, followed by Tukey's *post hoc* test, when a significant interaction was detected. Statistical significance at $p<0.05$ is indicated by *, $p<0.01$ by ** and $p<0.001$ by ***. Fold change values for *pomca* expression measured via qPCR were log transformed prior to analysis via two-way ANOVA, in order to meet the assumptions of the test (untransformed data is plotted).

Results

Zebrafish 21-hydroxylase (cyp21a2) is single copy gene

A single copy of the 21-hydroxylase gene, *cyp21a2*, was identified in the zebrafish. *cyp21a2* resides on chromosome 16 and has 2 predicted protein-coding splice variants, of 533 and 523 amino acids, each with 12 exons. Zebrafish cyp21a2 shares homology with other vertebrate CYP21 proteins. To determine the evolutionary conservation of the zebrafish Cyp21a2, protein sequence analysis was performed *in silico*. Zebrafish Cyp21a2 shares high sequence homology with other teleost fish and high sequence homology with the human 21-hydroxylase protein (40.71%) (**Supplementary Table 1**).

Temporo-spatial expression of the cyp21a2 gene

The expression of *the cyp21a2* gene was analysed by RT-PCR during early zebrafish development. The expression of *cyp21a2* started around the late segmentation period (28 hpf) and was maintained to 120 hpf (**Figure 1A**). Whole mount *in situ* hybridization (WISH) carried out at 24, 28 and 120 hpf, showed *cyp21a2* has high expression within the interrenal gland from 28 hpf (**Figure 1B**).

Generation of cyp21a2 null alleles in zebrafish using TALENs

To further study the function of 21-hydroxylase in zebrafish, we disrupted the *cyp21a2* gene employing a TALEN strategy. The TALEN binding sites were chosen within exon 2 to generate an early 5-prime disruption into the *cyp21a2* gene. The left TALEN targeted 17 nucleotides of the *cyp21a2* gene and the right TALEN targeted 20 nucleotides. Each was separated by a spacer sequence of 15 base pairs (**Supplementary Figure 1A**). The genomic disruption in injected embryos was confirmed by a BseYI restriction digest after PCR. Subsequently, three different heritable alleles were identified within the targeted spacer region of which two lines were maintained (*cyp21a2*^{uob2122} and *cyp21a2*^{uob2123}). The *cyp21a2*^{uob2122} mutant line has a 14 base pair deletion (c.del211-224) leading to a frameshift with a premature stop at amino-acid 96 (p.P70 *fs*26X). The second line carried a deletion of 13 nucleotides (c.del212-224) causing a frameshift and an early stop codon at position 83 (p.P70*fs*13X). Thus, both mutations are predicted to result in abolished 21-hydroxylase

function. Genotyping of wild-type, heterozygous and homozygous mutant larvae was performed by BseYI restriction digest after PCR (**Supplementary Figure 1B**).

Impaired VBA response and interrenal hyperplasia in cyp21a2 mutant larvae

The homozygous *cyp21a2* mutants were characterised during the first five days of zebrafish development to determine the requirement of cyp21a2 for steroid hormone biosynthesis in developing zebrafish larvae. *cyp21a2* homozygous mutants were morphologically similar to control siblings during this time (**Supplementary Figure 2A**). Since background adaptation in zebrafish has been associated with impaired glucocorticoid synthesis (18) and action (25), we subjected larvae to VBA analysis.

Larvae from a *cyp21a2* heterozygous in-cross were analysed by VBA assessment at 120 hpf and sorted into dark pigmentation and light pigmentation (**Supplementary Figure 2A**). Genotyping of 96 larvae (*cyp21a2*^{UOB2122} and *cyp21a2*^{UOB2123}) with impaired VBA revealed the vast majority of larvae were homozygous for the *cyp21a2* allele (**Supplementary Figure 2B**). Larvae capable of light adaptation were always either *cyp21a2* wild type (*cyp21a2*$^{+/+}$) or *cyp21a2* heterozygotes (*cyp21a2*$^{+/-}$). Only a small percentage of heterozygous *cyp21a2* $^{UOB2122/+}$ showed an altered VBA response confirming *cyp21a2* homozygous mutants can be reliably distinguished from their siblings by VBA assessment.

At 120 hpf, *cyp21a2* ^{UOB2122} homozygous larvae already showed an increased staining in the WISH analysis with an interrenal specific *cyp17a2* probe (**Figure 2A**). A quantitative analysis confirmed that interrenal size was significantly increased in homozygous mutants, compared to wild types and heterozygotes (**Figure 2B**). Interrenal hyperplasia was confirmed in the cyp21a2^{UOB2122} homozygous mutant larvae at 5 dpf using a 3D reconstruction of optical projection tomography (OPT) imaging of a WISH experiment with a *cyp17a2* probe (**Figure 2C**). This finding is most likely caused by ACTH-induced interrenal hyperplasia presenting the correlate of congenital adrenal hyperplasia in humans.

Impaired steroidogenesis in cyp21a2 mutant zebrafish

At 4 dpf, *cyp21a2*^{UOB2122} larvae were sorted into VBA+ and VBA- larvae (150 larvae each group) and samples were analysed at 5 dpf. The steroid hormone profiling by UPLC-MS/MS revealed detection of 17-hydroxyprogesterone in VBA- larvae only, and this did not further increase by stress treatment (**Figure 3A**). Remarkably, 21-deoxycortisol, which is pathognomonic for 21-hydroxylase deficiency in humans, was only detected at significant concentrations in VBA- larvae, biochemically proving 21-hydroxylase deficiency (**Figure 3B**). 21-deoxycortisol concentrations were not affected by stress treatment (**Figure 3B**). Additionally, UPLC/MSMS revealed reduced capability of VBA- larvae to produce cortisol (**Figure 3C**). Both VBA+ and VBA- larvae exhibited an increase in cortisol concentrations in response to acute stress (**Figure 3C**). We were not able to detect mineralocorticoid precursors such as deoxycorticosterone and corticosterone by LC/MSMS analysis nor did we detect androgen precursors such as androstenedione in VBA+ or VBA- zebrafish larvae (data not shown).

Systemic changes due to cortisol deficiency

The systemic effects of *cyp21a2* loss were analysed by quantitative RT-PCR. In response to the impaired interrenal cortisol biosynthesis, significantly increased levels of *pomca* transcripts were observed in VBA- larvae, when compared to VBA+ controls (**Figure 4A**), indicating activation of the HPI axis. Whilst pomca transcript levels in VBA+ larvae increased in response to acute stress, no stress-induced increase was detected in VBA- larvae, where levels were as high as stressed VBA+ larvae. These results were confirmed by WISH showing increased staining of pituitary tissue in *cyp21a2* homozygous mutants using a *pomca* probe, when compared to wild type larvae (**Supplementary Figure 3)**.

In addition, the expression of the glucocorticoid responsive gene *pck1* was significantly decreased in VBA- larvae compared to VBA+ controls (**Figure 4B**). Osmotic stress resulted in a significant increase of expression levels of *pck1* in VBA+ larvae, but did not have a significant effect on *pck1* levels in VBA- larvae (**Figure 4B**). Similarly, osmotic stress did not increase expression levels of *fkbp5* in VBA- larvae, whereas VBA+ larvae showed significantly increased expression levels under stress (**Figure 4C**). Overall, this clearly demonstrates reduced transcriptional response to stress on global level of VBA- larvae when compared to VBA+ larvae (**Figure 4A-C**).

Discussion

Zebrafish are increasingly employed as model organisms in biomedical research, including studying endocrine conditions, stress research as well as the modelling of anxiety and depression (26-28). The hypothalamic-pituitary-adrenal axis in mammals and the hypothalamic-pituitary-interrenal in fish play a crucial role in these scientific areas. However, the detailed biosynthetic pathway to cortisol in zebrafish remains partly elusive. Herein, we present clear *in vivo* evidence of the key role of 21-hydroxylase (Cyp21a2) in glucocorticoid biosynthesis in zebrafish larvae.

Some of the cytochrome P450 enzymes involved in steroid hormone biosynthesis such as P450 side chain cleavage (Cyp11a1 and Cyp11a2), 17-hydroxylase (Cyp17a1 and Cyp17a2) and P450 aromatase (Cyp19a1a and Cyp19a1b) remain duplicated and show a temporal-spatial or functional separation, whereas 3-beta-hydroxysteroid dehydrogenase (Hsd3b1) (29) and 11-hydroxylase (Cyp11c1) (30) exist as single copy genes. Similar to the latter genes, zebrafish have a single copy of the 21-hydroxylase gene (Cyp21a2), indicating that the duplicated copy arising from the whole genome duplication of the common teleost ancestor (31) has presumably been lost during evolution. An extensive database search did not reveal a second copy and zebrafish cyp21a2, which shows an overall homology to the human CYP21A2 orthologue of 41%, can therefore be assumed the functional gene in zebrafish.

Disruption of cyp21a2 leads to glucocorticoid deficiency

Expression of *cyp21a2* can be detected when the interrenal gland develops the ability of *de novo* cortisol synthesis (14). Significant expression of *cyp21a2* was mainly localized to the interrenal gland. By employing TALENs to disrupt the open-reading frame of *cyp21a2* we generated zebrafish mutant alleles with the loss of the conserved functional domains of 21-hydroxylase. A mutant line harboring a 14-base pair deletion was established and used to investigate the requirement of cyp21a2 for cortisol biosynthesis.

Visual background adaptation (VBA) is observed from 96hpf and is a rapid, reversible physiological process and is regulated by glucocorticoid receptor signaling in teleost fish (25). VBA involves the distribution or aggregation of melanin within the melanophore to blend into the surrounding environment (32). The VBA analysis of 5 dpf larvae subjected to lighter environments revealed that the overall majority of darker larvae correlated with zebrafish homozygous for the non-functional *cyp21a2*$^{-/-}$ genotype. In addition, homozygous cyp21a2$^{-/-}$ showed an upregulation of the HPI axis, as indicated by increased expression levels of the *pomca* gene assessed by qPCR and *in situ* hybridization. This finding is similar to humans with primary adrenal insufficiency, who show hyperpigmentation due to upregulation of the HPA axis with increased levels of POMC expression. Furthermore, this is consistent to observations in glucocorticoid-resistant (33) and glucocorticoid-deficient (18) zebrafish models leading to a disruption of the negative HPI feedback loop.

Cyp21a2 is a key enzyme in zebrafish cortisol biosynthesis

At 96 hpf larvae from heterozygous in-crosses were sorted according to their VBA response and collected at 120 hpf for steroid hormone analysis. VBA- larvae showed a pathognomonic

steroid hormone profile with increased concentrations of 17OHP and the 21OHD marker steroid hormone 21-deoxycortisol resembling the hormonal constellation of glucocorticoid precursors observed in humans with 21-hydroxylase deficiency (2). Cortisol was low under baseline conditions in VBA- larvae, and the cortisol response to osmotic stress by VBA- larvae did not reach that of baseline levels in VBA+ larvae. This was also observed on systemic level when assessing the expression levels of glucocorticoid responsive genes such as *pck1* and *fkbp5,* clearly indicating systemic glucocorticoid deficiency. However, overall cyp21a2-deficient mutants showed some residual ability to synthesize cortisol and, on systemic level, were less glucocorticoid deficient than our model of glucocorticoid deficiency due to disruption of the mitochondrial redox co-factor to steroidogenesis ferredoxin 1b (fdx1b) (18).

This observation has several possible explanations. Fdx1b deficiency affects enzymatic steps in the synthesis to glucocorticoids: the catalytic activity of Cyp11a2 and Cyp11c1. Furthermore, when collecting 150 larvae for each of the steroid hormone measurements, we cannot rule out that a proportion of heterozygous larvae might have been VBA -. However, we postulate the presence of another steroidogenic enzymes facilitating the residual 21-hydroxylation of the accumulating 17OHP in Cyp21a2-deficient larvae. The highly efficient interrenal 17-hydroxylase (Cyp17a2) (34) does most likely act as an alternative 21-hydroxylating enzyme in 21-hydroxylase deficient zebrafish larvae, as cyp17a2 has the ability *in vitro* to convert 17OHP to 11-deoxycortisol (personal communication Fred Guengerich). Thus, such a mechanism is the most likely explanation for measureable cortisol concentrations in Cyp21a2-deficient larvae.

Such a mechanism would also explain the residual cortisol synthesis leading the less pronounced systemic glucocorticoid deficiency indicated by measurable expression levels of glucocorticoid responsive genes *pck1* and *fkbp5*. Furthermore, the significant amounts of 21-deoxycortisol, detected in our mutants larvae, are likely to contribute as an additional factor, transactivating the expression of glucocorticoid responsive genes as has been demonstrated *in vitro* (5).

Cyp21a2-deficient zebrafish larvae as a model of glucocorticoid deficiency

In contrast to mice, zebrafish generate cortisol as the main glucocorticoid with the same intermediates as humans and follow as day active animals a similar circadian rhythm (13). Despite the fact that the murine deletion model of 21-hydroxylase have led to improved understanding of adrenal pathophysiology in CAH (8), it has been difficult to maintain homozygous murine *cyp21a2*-deletion models (6,8) making these an unsuitable tool to study systemic effects of 21-hydroxylase deficiency. Despite the lack of hyperandrogenism, our novel *in vivo* model of 21-hydroxylase deficiency resembles a significant number of key features of the human pathophysiology of 21OHD due to glucocorticoid deficiency. Thus, we believe that these mutant lines can be used to explore the whole organism response to cortisol deficiency due to 21OHD. It appears that during the developmental stages studied, Cyp21a2-deficient zebrafish larvae do not synthesise excess androgens despite producing increased amounts of 17OHP. Thus, it appears that androgen precursors cannot enter the androgen biosynthesis pathway. This suggests that Cyp17a2 lacking 17,20 lyase catalytic function (34) is the predominant active interrenal enzyme during the studied timeframe, and that Cyp17a1 might not be of significant functional relevance at 5 days post fertilisation. However, we believe that our novel *in vivo* model of 21-hydroxylase deficiency will be a useful tool to study the systemic consequences of cortisol deficiency modified by the systemic action of steroid hormone precursors such as 21-deoxycortisol.

In summary, we have employed a genetic engineering strategy to define a key step in glucocorticoid biosynthesis *in vivo*. By using molecular and biochemical approaches we characterized the role of Cyp21a2 during zebrafish development and showed that it is

required for interrenal cortisol synthesis. By using TALENs we have successfully generated *cyp21a2* mutant lines, disrupting the zebrafish steroid biosynthesis pathway, which was reflected in a steroid profile pathognomonic for 21-hydroxylase deficiency.

Our *cyp21a2* mutants will provide a valuable resource for exploring the impact of glucocorticoid deficiency and will provide novel insights into the regulation of other processes by steroid hormones including development, behavior and stress research.

Acknowledgement

We thank Silvia Parajes for helpful comments. We thank Michael Sandholzer for advice on OPT imaging.

Corresponding author: Nils Krone MD FRCPCH, Academic Unit of Child Health, Department of Oncology and Metabolism, University of Sheffield, Sheffield Children's Hospital, Western Bank, Sheffield S10 2TH, United Kingdom, Tel (+44) 0114 271 7508, Fax (+44) 0114 275 5364,
Email N.Krone@sheffield.ac.uk

This work was supported by the International Fund Congenital Adrenal Hyperplasia (2012 IFCAH research grant to N.K.), Medical Research Council Doctoral Training Partnerships studentship (A.G.), European Union 7th framework program Marie Curie Intra-European Fellowships PIEF-GA-2013–625827 (to M.W.) and PIEF-GA-2012-328959 (to T.G.), and a Society for Endocrinology (Early Career Grant to A.Z.)

Disclosure summary: Nothing to disclose

References

1. Krone N, Arlt W. Genetics of congenital adrenal hyperplasia. Best practice & research 2009; 23:181-192

2. Miller WL, Auchus RJ. The molecular biology, biochemistry, and physiology of human steroidogenesis and its disorders. Endocr Rev 2011; 32:81-151

3. Reisch N, Arlt W, Krone N. Health problems in congenital adrenal hyperplasia due to 21-hydroxylase deficiency. Hormone research in paediatrics 2011; 76:73-85

4. Arlt W, Krone N. Adult Consequences of Congenital Adrenal Hyperplasia. Horm Res 2007; 68:158-164

5. Pijnenburg-Kleizen KJ, Engels M, Mooij CF, Griffin A, Krone N, Span PN, van Herwaarden AE, Sweep FC, Claahsen-van der Grinten HL. Adrenal Steroid Metabolites Accumulating in Congenital Adrenal Hyperplasia Lead to Transactivation of the Glucocorticoid Receptor. Endocrinology 2015; 156:3504-3510

6. Riepe FG, Tatzel S, Sippell WG, Pleiss J, Krone N. Congenital Adrenal Hyperplasia: The Molecular Basis of 21-Hydroxylase Deficiency in H-2aw18 Mice. Endocrinology 2005; 146:2563-2574

7. Gotoh H, Kusakabe M, Shiroishi T, Moriwaki K. Survival of steroid 21-hydroxylase-deficient mice without endogenous corticosteroids after neonatal treatment and genetic rescue by transgenesis as a model system for treatment of congenital adrenal hyperplasia in humans. Endocrinology 1994; 135:1470-1476.

8. Bornstein SR, Tajima T, Eisenhofer G, Haidan A, Aguilera G. Adrenomedullary function is severely impaired in 21-hydroxylase- deficient mice. Faseb J 1999; 13:1185-1194.

9. McGonnell IM, Fowkes RC. Fishing for gene function--endocrine modelling in the zebrafish. The Journal of endocrinology 2006; 189:425-439

10. To TT, Hahner S, Nica G, Rohr KB, Hammerschmidt M, Winkler C, Allolio B. Pituitary-interrenal interaction in zebrafish interrenal organ development. Mol Endocrinol 2007; 21:472-485

11. Alsop D, Vijayan MM. Molecular programming of the corticosteroid stress axis during zebrafish development. Comparative biochemistry and physiology 2009; 153:49-54
12. Steenbergen PJ, Richardson MK, Champagne DL. The use of the zebrafish model in stress research. Progress in neuro-psychopharmacology & biological psychiatry 2011; 35:1432-1451
13. Dickmeis T. Glucocorticoids and the circadian clock. The Journal of endocrinology 2009; 200:3-22
14. Alsop D, Vijayan MM. Development of the corticosteroid stress axis and receptor expression in zebrafish. American journal of physiology 2008; 294:R711-719
15. Kimmel CB, Ballard WW, Kimmel SR, Ullmann B, Schilling TF. Stages of embryonic development of the zebrafish. Dev Dyn 1995; 203:253-310
16. Dereeper A, Guignon V, Blanc G, Audic S, Buffet S, Chevenet F, Dufayard JF, Guindon S, Lefort V, Lescot M, Claverie JM, Gascuel O. Phylogeny.fr: robust phylogenetic analysis for the non-specialist. Nucleic acids research 2008; 36:W465-469
17. Dereeper A, Audic S, Claverie JM, Blanc G. BLAST-EXPLORER helps you building datasets for phylogenetic analysis. BMC Evol Biol 2010; 10:8
18. Griffin A, Parajes S, Weger M, Zaucker A, Taylor AE, O'Neil DM, Muller F, Krone N. Ferredoxin 1b (Fdx1b) is the essential mitochondrial redox partner for cortisol biosynthesis in zebrafish. Endocrinology 2016; 157:1122-1134
19. Thisse C, Thisse B. High-resolution in situ hybridization to whole-mount zebrafish embryos. Nat Protoc 2008; 3:59-69
20. Muthu V, Eachus H, Ellis P, Brown S, Placzek M. Rx3 and Shh direct anisotropic growth and specification in the zebrafish tuberal/anterior hypothalamus. Development (Cambridge, England) 2016; 143:2651-2663
21. Doyle EL, Booher NJ, Standage DS, Voytas DF, Brendel VP, VanDyk JK, Bogdanove AJ. TAL Effector-Nucleotide Targeter (TALE-NT) 2.0: tools for TAL effector design and target prediction. Nucleic acids research 2012; 40:W117-W122
22. O'Reilly MW, Kempegowda P, Jenkinson C, Taylor AE, Quanson JL, Storbeck KH, Arlt W. 11-Oxygenated C19 Steroids Are the Predominant Androgens in Polycystic Ovary Syndrome. J Clin Endocrinol Metab 2017; 102:840-848
23. Willems E, Leyns L, Vandesompele J. Standardization of real-time PCR gene expression data from independent biological replicates. Anal Biochem 2008; 379:127-129
24. Wong MD, Dazai J, Walls JR, Gale NW, Henkelman RM. Design and implementation of a custom built optical projection tomography system. PLoS One 2013; 8:e73491
25. Muto A, Taylor MR, Suzawa M, Korenbrot JI, Baier H. Glucocorticoid receptor activity regulates light adaptation in the zebrafish retina. Frontiers in neural circuits 2013; 7:145
26. Stewart AM, Braubach O, Spitsbergen J, Gerlai R, Kalueff AV. Zebrafish models for translational neuroscience research: from tank to bedside. Trends in neurosciences 2014; 37:264-278
27. Stewart AM, Ullmann JF, Norton WH, Parker MO, Brennan CH, Gerlai R, Kalueff AV. Molecular psychiatry of zebrafish. Molecular psychiatry 2015; 20:2-17
28. Richendrfer H, Pelkowski SD, Colwill RM, Creton R. On the edge: pharmacological evidence for anxiety-related behavior in zebrafish larvae. Behav Brain Res 2012; 228:99-106
29. Lin JC, Hu S, Ho PH, Hsu HJ, Postlethwait JH, Chung BC. Two Zebrafish hsd3b Genes Are Distinct in Function, Expression, and Evolution. Endocrinology 2015; 156:2854-2862

30. Wilson KS, Matrone G, Livingstone DE, Al-Dujaili EA, Mullins JJ, Tucker CS, Hadoke PW, Kenyon CJ, Denvir MA. Physiological roles of glucocorticoids during early embryonic development of the zebrafish (Danio rerio). J Physiol 2013; 591:6209-6220
31. Postlethwait JH, Yan YL, Gates MA, Horne S, Amores A, Brownlie A, Donovan A, Egan ES, Force A, Gong Z, Goutel C, Fritz A, Kelsh R, Knapik E, Liao E, Paw B, Ransom D, Singer A, Thomson M, Abduljabbar TS, Yelick P, Beier D, Joly JS, Larhammar D, Rosa F, Westerfield M, Zon LI, Johnson SL, Talbot WS. Vertebrate genome evolution and the zebrafish gene map. Nature genetics 1998; 18:345-349
32. Logan DW, Burn SF, Jackson IJ. Regulation of pigmentation in zebrafish melanophores. Pigment cell research / sponsored by the European Society for Pigment Cell Research and the International Pigment Cell Society 2006; 19:206-213
33. Ziv L, Muto A, Schoonheim PJ, Meijsing SH, Strasser D, Ingraham HA, Schaaf MJ, Yamamoto KR, Baier H. An affective disorder in zebrafish with mutation of the glucocorticoid receptor. Molecular psychiatry 2013; 18:681-691
34. Pallan PS, Nagy LD, Lei L, Gonzalez E, Kramlinger VM, Azumaya CM, Wawrzak Z, Waterman MR, Guengerich FP, Egli M. Structural and kinetic basis of steroid 17alpha,20-lyase activity in teleost fish cytochrome P450 17A1 and its absence in cytochrome P450 17A2. The Journal of biological chemistry 2015; 290:3248-3268

Figure 1 Zebrafish *cyp21a2* expression is largely restricted to the interrenal gland. A) Analysis of *cyp21a2* expression during embryonic and early larval development by RT-PCR with *bactin1* as an internal standard (gel images inversed). A no template control sample (NTC) served as negative control. The onset of detectable *cyp21a2* expression is at 28 hpf, after which *cyp21a2* continues to be expressed at all stages examined. B) Images of wild type larvae at different stages after whole-mount RNA-*in situ* hybridisation against *cyp21a2*. Left panels show lateral view, with head to the left, right panels show a dorsal view. No staining is seen in 24 hpf embryos. In 28 hpf embryos and 120 hpf larvae, strong staining is observed in the interrenal gland region, with some faint signal detected at 120 hpf in the head (arrows). Scale bar: 0.1 mm.

Figure 2 Zebrafish *cyp21a2* mutants have enlarged interrenal tissue at 120 hpf. A) Expression of *cyp17a2* in 120 hpf *cyp21a2*^{uob2122} wild type, heterozygous and homozygous *cyp21a2*^{uob2122} mutant larvae in lateral (upper panel) and dorsal (lower panel) views. The area of *cyp17a2* positive interrenal tissue (arrows) is enlarged in homozygous mutants. N= 6 each. Scale bar: 0.25 mm. B) Quantification of the area of *cyp17a2* positive interrenal tissue in 120 hpf *cyp21a2*^{uob2122} larvae. The size of the interrenal tissue is significantly larger in homozygous mutants (Mut), compared to wild type (WT) and heterozygous (Het) siblings (ANOVA; F=12.15, df=2,15, p=0.0007; Tukey; WT vs Het p=0.895, WT vs mut p=0.003, Het vs Mut p=0.003). **, p<0.01 compared to wild types and heterozygotes. N=4-8 each. C) OPT imaging of 120 hpf cyp21a2 larvae after WISH for cyp17a2 reveals an enlarged interrenal gland in cyp21a2^{uob2122} homozygous mutants (right) compared with wild type siblings (left). Whole mount views for ventral (upper), lateral (middle) and dorsal (lower) are shown.

Figure 3 Zebrafish *cyp21a2* mutants have impaired steroidogenesis. Measurement of baseline and stress-induced concentrations of steroid hormones in 120 hpf *cyp21a2*^{uob2122} VBA+ (wild type) and VBA- (mutant) larvae by UPLC/MSMS. A) 17-hydroxyprogesterone concentrations are significantly increased in VBA- (mutant) larvae, compared to VBA+ (wild type) larvae and levels are not significantly altered by stress treatment (two-way ANOVA; Genotype F=29.71, df=1,8, p=0.0006, Stress F=0.68, df=1,8, p=0.433, genotype: stress

F=0.68, df=1,8, p=0.433). N= 3 each. B) 21-deoxycortisol concentration is significantly increased in VBA- (mutant) larvae, compared to VBA+ (wild type) larvae and is not significantly altered by stress treatment (two-way ANOVA; Genotype F=9.97, df=1,8, p=0.013, Stress F=0.36, df=1,8, p=0.565, genotype: stress F=1.08, df=1,8, p=0.329). N= 3 each. C) Cortisol concentration is significantly reduced in VBA- (mutant) larvae, compared to VBA+ (wild type) larvae and levels are significantly increased by stress treatment (ANOVA; Genotype F=28.63, df=1,8, p=0.0007, Stress F=10.19, df=1,8, p=0.013, genotype: stress F=2.35, df=1,8, p=0.163). N= 3 each.

Figure 4 Zebrafish *cyp21a2* mutants have a dysregulated HPI-axis. Analysis of baseline and stress-induced transcript levels of *pomca, fkbp5, pck1* in 120 hpf VBA+ (wild type) versus their VBA- (mutant) siblings by qPCR. Expression is relative to the control gene *gapdh*. A) Expression of *pomca* is affected by VBA response (genotype) and stress treatment (two-way ANOVA, VBA: stress interaction, F=4.15, df=1,20, p=0.05). Expression increases in VBA+ larvae in response to stress (p=0.01) and expression in VBA- larvae under control (p=0.007) and stressed (p=0.002) conditions is higher than VBA+ baseline levels. Analysis carried out on log-transformed data, untransformed data is plotted. N= 6 each. B) Expression of *pck1* is effected by VBA response and stress treatment (two-way ANOVA, VBA: stress interaction, F=9.59, df=1,16, p=0.006). Expression is reduced in VBA- larvae compared to VBA+ larvae under baseline (p=0.005) and stressed (p<0.0001) conditions. Expression increases in VBA+ larvae in response to stress (p<0.0001), but stress has no effect on expression levels in VBA- larvae (p=0.18). N= 5 each. C) Expression of *fkbp5* is effected by VBA response and stress treatment (two-way ANOVA, VBA: stress interaction, F=11.38, df=1,16, p=0.003). Expression in VBA+ larvae increases in response to stress (p=0.005), but stress has no effect on VBA- expression levels (p=0.84). fkbp5 expression in VBA+ larvae under stress was significantly lower in VBA- compared with VBA+ larvae. (p=0.0001). N= 5 each.

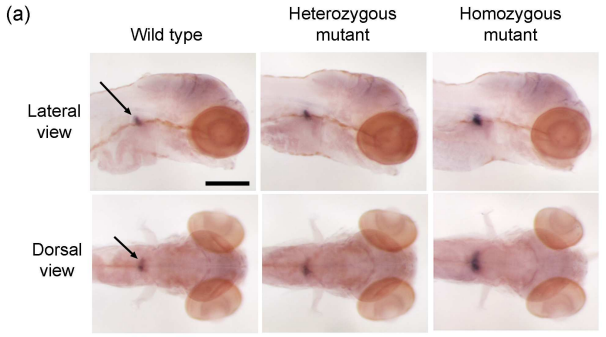

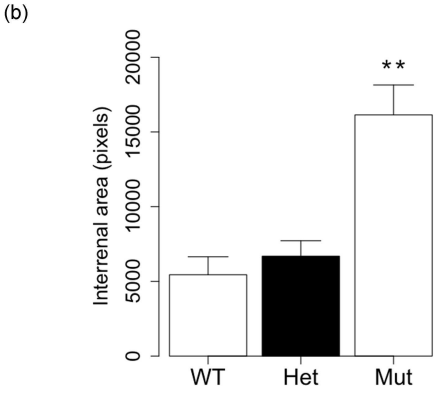

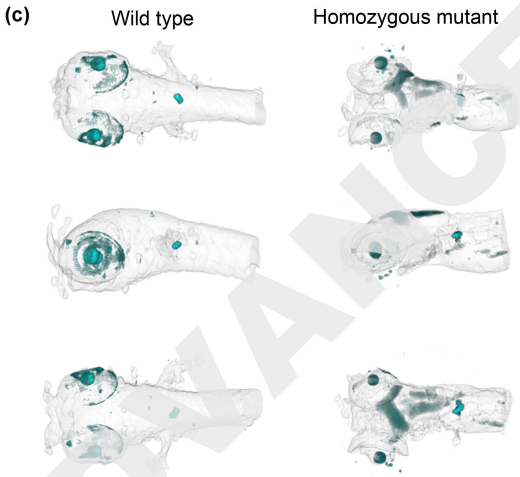

(a)

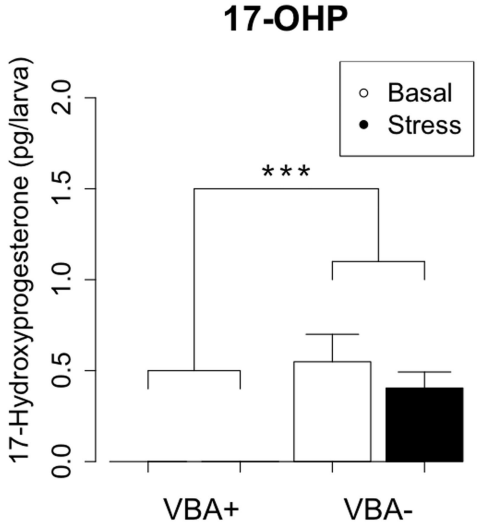

(b)

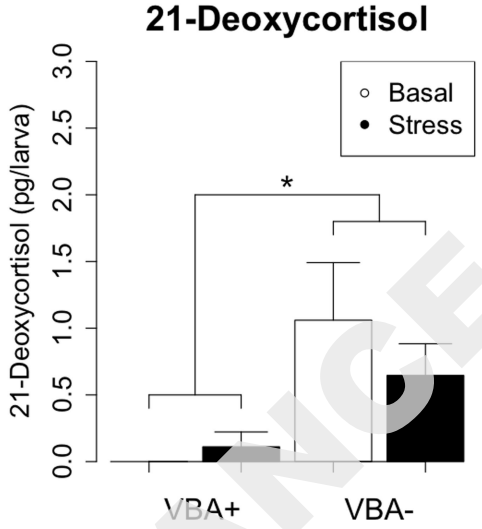

(c)